Inorganic Chemistry
Article

Inorg. Chem. **2009**, *48*, 6425–6435 **6425**
DOI: 10.1021/ic900149v

Emission Enhancement through Dual Donor Sensitization: Modulation of Structural and Spectroscopic Properties in a Series of Europium Tetracyanoplatinates

Branson A. Maynard,[†] Philip A. Smith,[†] LeAnn Ladner,[†] Ayesha Jaleel,[†] Nuquie Beedoe,[‡] Carlos Crawford,[‡] Zerihun Assefa,*[,‡] and Richard E. Sykora*[,†]

[†]*Department of Chemistry, University of South Alabama, Mobile, Alabama 36688, and* [‡]*Department of Chemistry, North Carolina A&T State University, Greensboro, North Carolina 27411*

Received January 22, 2009

The synthesis of three different europium tetracyanoplatinates all incorporating 2,2′:6′,2″-terpyridine (terpy) have been carried out in acetonitrile/water mixtures by reaction of Eu^{3+} salts with terpy and potassium tetracyanoplatinate. The use of different Eu^{3+} sources results in the isolation of $Eu(C_{15}H_{11}N_3)(H_2O)_2(NO_3)(Pt(CN)_4)\cdot CH_3CN$ (**1**), $\{Eu(C_{15}H_{11}N_3)(H_2O)_3\}_2(Pt(CN)_4)_3\cdot 2H_2O$ (**2**), or $[Eu(C_{15}H_{11}N_3)(H_2O)_2(CH_3COO)_2]_2Pt(CN)_4\cdot 3H_2O$ (**3**) for the nitrate, triflate, or acetate salts, respectively. All three compounds have been prepared as colorless crystals, and single-crystal X-ray diffraction has been used to investigate their structural features. Crystallographic data (Mo$K\alpha$, $\lambda = 0.71073$ Å, $T = 290$ K): **1**, monoclinic, space group $P2_1/c$, $a = 12.835(1)$, $b = 15.239(1)$, $c = 13.751(2)$ Å, $\beta = 105.594(9)°$, $V = 2590.8(5)$ Å^3, $Z = 4$; **2**, triclinic, space group $P\bar{1}$, $a = 9.1802(8)$ Å, $b = 10.8008(9)$ Å, $c = 13.5437(9)$ Å, $\alpha = 84.491(6)°$, $\beta = 75.063(7)°$, $\gamma = 79.055(7)°$, $V = 1272.4(2)$ Å^3, $Z = 1$; **3**, triclinic, space group $P\bar{1}$, $a = 12.110(3)$ Å, $b = 12.7273(11)$ Å, $c = 18.7054(16)$ Å, $\alpha = 92.859(7)°$, $\beta = 92.200(11)°$, $\gamma = 118.057(10)°$, $V = 2534.8(7)$ Å^3, $Z = 2$. Variation of the counteranions in these systems provides the opportunity to modify the structures and coordination environment of Eu^{3+} for **1**−**3.** Compounds **1** and **2** are both one-dimensional, polymeric compounds that contain Eu^{3+} ions chelated by terpy and bridged by tetracyanoplatinate anions. **3** is a zero-dimensional complex salt in which Eu^{3+} is coordinated by terpy, acetate, and water, but not tetracyanoplatinate. The structural differences result in varying sensitization phenomena for the three compounds. Compounds **1** and **2** display efficient donor−acceptor intramolecular energy transfer (IET) where dual donor species, terpyridine and tetracyanoplatinate, simultaneously enhance the acceptor Eu^{3+} emission. In both compounds the donor species are directly coordinated to the acceptor ion, and hence a highly efficient dual-donor effect is exhibited for the IET mechanisms. In **3** where only the terpy ligand is directly coordinated to Eu^{3+}, the sensitization involves only one donor species. The $Pt(CN)_4^{2-}$ unit in **3**, which lacks direct bonding to Eu^{3+}, exhibits strong emission indicating the lack of cooperative enhancement of the lanthanide emission.

Introduction

The optical properties of the tetracyanoplatinates (TCPs), $M_x[Pt(CN)_4]_y\cdot nH_2O$ (M = alkali, alkaline earth) were observed as early as 1822.[1] Since then more comprehensive studies have been made on the optical[2−5] and structural[5−7] properties of TCP compounds containing a number of different cations. The absorption and luminescence properties of many TCP compounds have been studied in detail in a variety of salts with alkali metal,[4,8−10] alkaline earth metal,[4,8,11,12] and lanthanide[7,13−16] cations, as well as in fluid solutions.[17,18] A common feature in the structural chemistry of the TCP

*To whom correspondence should be addressed. E-mail: rsykora@jaguar1.usouthal.edu (R.E.S.), zassefa@ncat.edu (Z.A.). Phone: (251) 460-7422 (R.E.S.), (336) 285-2255 (Z.A.).

(1) Gmelin, L. *Jahrbuch der Chemie und Physik* **1822**, *36*, 230.
(2) Yamada, S. *J. Am. Chem. Soc.* **1951**, *73*, 1182–1184.
(3) Tolstoi, N. A.; Tofimov, A. K.; Tkachuk, A. M. *Bull. Acad. of Sci. USSR. Phys. Ser.* **1956**, *20*, 529–535.
(4) (a) Gliemann, G.; Yersin, H. *Struct. Bonding (Berlin)* **1985**, *62*, 87–153 and references therein. (b) Yersin, H.; Gliemann, G. *Ann. N.Y. Acad. Sci.* **1978**, *313*, 539–559.
(5) Moreau-Colin, M. L. *Struct. Bonding (Berlin)* **1972**, *10*, 167–190.
(6) Holzapfel, W.; Yersin, H.; Gliemann, G. *Z. Kristallogr.* **1981**, *157*, 47–67 and references therein.
(7) (a) Loosli, A.; Wermuth, M.; Güdel, H.-U.; Capelli, S.; Hauser, J.; Bürgi, H.-B. *Inorg. Chem.* **2000**, *39*, 2289–2293. (b) Daniels, W.; Yersin, H.; Von Philipsborn, H.; Gliemann, G. *Solid State Commun.* **1979**, *30*, 353–355.
(8) Hidvegi, I.; von Ammon, W.; Gliemann, G. *J. Chem. Phys.* **1982**, *76*, 4361–4369.
(9) Cornelius, J. B.; Trapp, R. M.; Delord, T. J.; Fronczek, F. R.; Watkins, S. F.; Orosz, J. J.; Musselman, R. L. *Inorg. Chem.* **2003**, *42*, 3026–3035.
(10) Yersin, H.; Riedl, U. *Inorg. Chem.* **1995**, *34*, 1642–1645.
(11) Clark, S.; Day, P.; Huddart, D. J.; Ironside, C. N. *J. Chem. Soc., Faraday Trans. 2: Mol. Chem. Phys.* **1983**, *79*, 65–76.
(12) Day, P.; Ferguson, J. J. *Chem. Soc., Faraday Trans. 2: Mol. Chem. Phys.* **1981**, *77*, 1579–1588.
(13) Yersin, H.; Stock, M. *J. Chem. Phys.* **1982**, *76*, 2136–2138.
(14) von Ammon, W.; Hidvegi, I.; Gliemann, G. *J. Chem. Phys.* **1984**, *80*, 2837–2844.
(15) Yersin, H. *J. Chem. Phys.* **1978**, *68*, 4707–4713.
(16) von Ammon, W.; Gliemann, G. *J. Chem. Phys.* **1982**, *77*, 2266–72.
(17) (a) Schindler, J. W.; Fukuda, R. C.; Adamson, A. W. *J. Am. Chem. Soc.* **1982**, *104*, 3596–3600. (b) Schindler, J. W.; Fukuda, R. C.; Adamson, A. W. Report **1981**, (TR-16; Order No. AD-A105675), p 33.
(18) Lechner, A.; Gliemann, G. *J. Am. Chem. Soc.* **1989**, *111*, 7469–7475.

Published on Web 06/17/2009

crystals is the presence of pseudo-one-dimensional (1-D) columnar chains[4a,6] of planar TCP anions stacked parallel to one another. The significant Pt−Pt interactions that occur between the adjacent TCP anions in these chains, from ∼3 to 3.7 Å,[6] provide highly tunable spectral properties.[4a,7a,13] Experiments have shown that the Pt−Pt distances, and hence the associated spectroscopic properties, can be tuned by chemical and physical variations such as by the choice of countercation[16,19] or applied pressure.[10,13,18−20] It has also been shown in $Ln_2[Pt(CN)_4]_3 \cdot 18H_2O$ (Ln = Sm, Eu) that tetracyanoplatinate excitation can be transferred non-radiatively to the Sm^{3+} or Eu^{3+} ions,[13,15,20] respectively, resulting in emission from these cations.

More recently, investigations into the catalytic and magnetic properties of TCP compounds have gained focus. Shore et al. have prepared a number of lanthanide TCP, as well as tetracyanonickelate and tetracyanopalladate, compounds in *N*,*N*-dimethylformamide (DMF) or *N*,*N*-dimethylacetamide (DMA) solutions such as $\{(DMF)_{10}Ln_2[M(CN)_4]_3\}_\infty$ (Ln = Y, Sm, Eu, Yb; M = Ni, Pd, Pt),[21] $\{[NH_4](DMF)_4Yb[Pt(CN)_4]_2\}_\infty$,[22] and $\{(DMA)_4Yb[Ni(CN)_4]Cl\}_\infty$[21c] The Shore group has demonstrated that several of these compounds can be used as bimetallic catalytic precursors to prepare very active heterogeneous catalysts.[23] For example, a Yb−Pd bimetallic catalyst supported on SiO_2, prepared from type B $\{(DMF)_{10}Yb_2[Pd(CN)_4]_3\}_\infty$, is more active toward the hydrogenation of phenol than supported Pd alone.[23b] The magnetism of cyanide-bridged lanthanide/transition metal bimetallic compounds has also been investigated. For example, ferromagnetic coupling between Sm^{3+} and Fe^{3+} was reported in $\{[Sm(tptz)(H_2O)_4Fe(CN)_6 \cdot 8H_2O\}_\infty$[24] (tptz = 2,4,6-tri(2-pyridyl)-1,3,5-triazine). Other reports have also focused on the synthesis and magnetism of compounds containing Ln^{3+} centers bridged by hexacyanometallate[25] anions, while fewer magnetic reports have surfaced on lanthanide compounds containing tetracyanometallate[26,27] anions.

Our interests lie in the production of novel lanthanide compounds containing chromophoric ligands that photosensitize lanthanide-ion luminescence. Compounds of this sort are of intense current interest and can be used in technological applications such as fluoroimmunoassays,[28,29] cellular imaging,[30] chemosensors,[31] optical communications,[32,33] and optoelectronic devices.[34] The usual impediment in lanthanide ion systems is that direct absorption of the f-f excited states is very inefficient. Hence, a light harvesting ligand is essential to enhance the emission from the metal cation site. Donor ligands used for such applications usually have strong absorbance in the UV region and transfer their excited energy to the acceptor lanthanide ions.[35−37] The tetracyanoplatinate system comprises one such donor system that has been shown to meet these criteria.[13,15,20] Another donor system that absorbs in the UV and has been shown to undergo energy transfer processes with select lanthanide cations is the 2,2′:6′,2″-terpyridine (terpy) system; a number of compounds have been reported that contain terpy, or derivatives thereof, that act as light harvesting antennae and can subsequently transfer absorbed energy to coordinated Ln^{3+} cations.[35,38] One of our research aims is to prepare compounds that contain multiple donor species that can cooperatively enhance the lanthanide emission. In doing so we hope to (1) broaden the energy range for donor light harvesting and (2) create systems with highly efficient lanthanide luminescence via cooperative energy transfer from the donor groups.

We recently reported our preliminary findings in this area, which described the synthesis, structure, and spectroscopic properties of the polymeric compound, $Eu(C_{15}H_{11}N_3)(H_2O)_2(NO_3)(Pt(CN)_4) \cdot CH_3CN$ (**1**).[39] Herein we present further evidence for the intramolecular energy transfer (IET) process observed in this compound. Two additional europium tetracyanoplatinates incorporating terpy, $\{Eu(C_{15}H_{11}N_3)(H_2O)_3\}_2(Pt(CN)_4)_3 \cdot 2H_2O$ (**2**) and $[Eu(C_{15}H_{11}N_3)(H_2O)_2(CH_3COO)_2]_2Pt(CN)_4 \cdot 3H_2O$ (**3**), have since been synthesized by changing the counteranions of the Eu^{3+} salts used in the syntheses. In this report we compare and contrast

(19) Yersin, H.; Hidvegi, I.; Gliemann, G.; Stock, M. *Phys. Rev. B: Condens. Matter Mater. Phys.* **1979**, *19*, 177–180.
(20) Yersin, H.; von Ammon, W.; Stock, M.; Gliemann, G. *J. Lumin.* **1979**, *18−19*, 774–778.
(21) (a) Du, B.; Ding, E.; Meyers, E. A.; Shore, S. G. *Inorg. Chem.* **2001**, *40*, 3637–3638. (b) Liu, J.; Knoeppel, D. W.; Liu, S.; Meyers, E. A.; Shore, S. G. *Inorg. Chem.* **2001**, *40*, 2842–2850. (c) Knoeppel, D. W.; Liu, J.; Meyers, E. A.; Shore, S. G. *Inorg. Chem.* **1998**, *37*, 4828–4837. (d) Knoeppel, D. W.; Shore, S. G. *Inorg. Chem.* **1996**, *35*, 1747–1748. (e) Plecnik, C. E.; Liu, S.; Shore, S. G. *Acc. Chem. Res.* **2003**, *36*, 499–508.
(22) Du, B.; Meyers, E. A.; Shore, S. G. *Inorg. Chem.* **2001**, *40*, 4353–4360.
(23) (a) Rath, A.; Aceves, E.; Mitome, J.; Liu, J.; Ozkan, U. S.; Shore, S. G. *J. Mol. Catal. A: Chem.* **2001**, *165*, 103–111. (b) Liu, S.; Poplaukhin, P; Ding, E.; Plecnik, C. E.; Chen, X.; Keane, M. A.; Shore, S. G. *J. Alloys Compd.* **2006**, *418*, 21–26. (c) Jujjuri, S.; Ding, E.; Shore, S. G.; Keane, M. A. *J. Mol. Catal. A: Chem.* **2007**, *272*, 96–107.
(24) Zhao, H.; Lopez, N.; Prosvirin, A.; Chifotides, H. T.; Dunbar, K. R. *Dalton Trans.* **2007**, 878–888.
(25) (a) Figuerola, A.; Diaz, C.; El Fallah, M. S.; Ribas, J.; Maestro, M.; Mahia, J. *Chem. Commun.* **2001**, 1204–1205. (b) Figuerola, A.; Ribas, J.; Llunell, M.; Casanova, D.; Maestro, M.; Alvarez, S.; Diaz, C. *Inorg. Chem.* **2005**, *44*, 6939–6948. (c) Koner, R.; Drew, M. G. B.; Figuerola, A.; Diaz, C.; Mohanta, S. *Inorg. Chim. Acta* **2005**, *358*, 3041–3047. (d) Figuerola, A.; Ribas, J.; Solans, X.; Font-Bardia, M.; Maestro, M.; Diaz, C. *Eur. J. Inorg. Chem.* **2006**, 1846–1852.
(26) Du, B.; Shore, S. G.; Ebels, U. S.; Wigen, P. E. Book of Abstracts, 216th ACS National Meeting, Boston, MA, **1998**, INOR-596.
(27) Du, B., Ph.D. Dissertation, The Ohio State University, Columbus, Ohio, 2000, p 427.
(28) Barnard, G. *Immunodiagnostics* **1999**, 137–158.
(29) Nanda, S.; Guardigli, M.; Manet, I.; Ziessel, R.; Lehn, J.-M. *Med., Biol., Environ.* **1995**, *23*(1), 101–107.
(30) Poole, R. A.; Montgomery, C. P.; New; Elizabeth, J.; Congreve, A.; Parker, D.; Botta, M. *Org. Biomol. Chem.* **2007**, *5*(13), 2055–2062.
(31) Brunet, E.; Juanes, O.; Rodriguez-Ubis, J. C. *Curr. Chem. Biol.* **2007**, *1*(1), 11–39.
(32) Zang, F. X.; Li, W. L.; Hong, Z. R.; Wei, H. Z.; Li, M. T.; Sun, X. Y.; Lee, C. S. *Appl. Phys. Lett.* **2004**, *84*(25), 5115–5117.
(33) Zang, F. X.; Hong, Z. R.; Li, W. L.; Li, M. T.; Sun, X. Y. *Appl. Phys. Lett.* **2004**, *84*(14), 2679–2681.
(34) Okada, K.; Wang, Y.-F.; Chen, T.-M.; Kitamura, M.; Nakaya, T. *J. Mater. Chem.* **1999**, *9*(12), 3023–3026.
(35) (a) Gunnlaugsson, T.; Stomeo, F. *Org. Biomol. Chem.* **2007**, *5*, 1999−2009 and references therein. (b) Eliseeva, S. V.; Kotova, O. V.; Gumy, F.; Semenov, S. N.; Kessler, V. G.; Lepnev, L. S.; Bunzli, J.-C. G.; Kuzmina, N. P. *J. Phys. Chem. A* **2008**, *112*(16), 3614–26.
(36) Xu, H.-B.; Shi, L.-X.; Ma, E.; Zhang, L.-Y.; Wei, Q.-H.; Chen, Z.-N. *Chem. Commun.* **2006**, 1601–1603.
(37) Coppo, P.; Duati, M.; Kozhevnikov, V. N.; Hofstraat, J. W.; DeCola, L. *Angew. Chem., Int. Ed.* **2005**, *44*, 1806–1810.
(38) (a) Bekiari, V.; Lianos, P. *J. Lumin.* **2003**, *101*, 135–140. (b) Ziessel, R. F.; Ulrich, G.; Charbonnière, L.; Imbert, D.; Scopelliti, R.; Bünzli, J.-C. G. *Chem.—Eur. J.* **2006**, *12*, 5060–5067. (c) Mukkala, V.-M.; Takalo, H.; Liitti, P.; Hemmilä, I. *J. Alloys Compd.* **1995**, *225*, 507–510. (d) Tong, B.-H.; Wang, S.-J.; Jiao, J.; Ling, F.-R.; Meng, Y.-Z.; Wang, B. *J. Photochem. Photobiol., A* **2007**, *191*, 74–79. (e) Viswanathan, S.; de Bettencourt-Dias, A. Abstracts of Papers, 232nd ACS National Meeting, San Francisco, CA, **2006**, INOR-725.
(39) Maynard, B. A.; Kalachnikova, K.; Whitehead, K.; Assefa, Z.; Sykora, R. E. *Inorg. Chem.* **2008**, *47*, 1895–1897.

Table 1. Crystallographic Data for $Eu(C_{15}H_{11}N_3)(H_2O)_2(NO_3)(Pt(CN)_4)\cdot CH_3CN$ (**1**), $\{Eu(C_{15}H_{11}N_3)(H_2O)_3\}_2(Pt(CN)_4)_3\cdot 2H_2O$ (**2**), and $[Eu(C_{15}H_{11}N_3)(H_2O)_2(CH_3COO)_2]_2Pt(CN)_4\cdot 3H_2O$ (**3**)

compound	**1**	**2**	**3**
formula	$C_{21}H_{18}EuN_9O_5Pt$	$C_{42}H_{38}Eu_2N_{18}O_8Pt_3$	$C_{42}H_{48}Eu_2N_{10}O_{15}Pt$
formula weight (amu)	823.49	1812.10	1431.91
space group	$P2_1/c$ (No. 14)	$P\bar{1}$ (No. 2)	$P\bar{1}$ (No. 2)
a (Å)	12.8353(14)	9.1802(8)	12.110(3)
b (Å)	15.2394(13)	10.8008(9)	12.7273(11)
c (Å)	13.7512(16)	13.5437(9)	18.7054(16)
α (deg)	90	84.491(6)	92.859(7)
β (deg)	105.594(9)	75.063(7)	92.200(11)
γ (deg)	90	79.055(7)	118.057(10)
V (Å^3)	2590.8(5)	1272.4(2)	2534.8(7)
Z	4	1	2
T (K)	290	290	290
λ (Å)	0.71073	0.71073	0.71073
ρ_{calcd} (g cm^{-3})	2.111	2.365	1.876
μ(Mo $K\alpha$) (mm^{-1})	7.842	10.714	5.270
$R(F_o)$ for $F_o^2 > 2\sigma(F_o^2)^a$	0.0297	0.0339	0.0385
$R_w(F_o^2)^b$	0.0781	0.0943	0.1123

^{a} $R(F_o) = \sum||F_o| - |F_c||/\sum|F_o|$. ^{b} $R_w(F_o^2) = [\sum w(F_o^2 - F_c^2)^2/\sum wF_o^4]^{1/2}$.

the structures and IET processes of these three europium tetracyanoplatinates.

Experimental Section

Materials and Methods. $Eu(NO_3)_3\cdot 6H_2O$ (Alfa Aesar, 99.9%), $Eu(CF_3SO_3)_3\cdot xH_2O$ (Alfa Aesar, 98%), $Eu(CH_3COO)_3\cdot xH_2O$ (Alfa Aesar, 99.9%), 2,2′:6′,2″-terpyridine (Alfa Aesar, 97%), and $K_2Pt(CN)_4\cdot 3H_2O$ (Alfa Aesar, 99.9%) were used for the syntheses as received without further purification. The reaction conditions given below produced the highest yields of the respective compounds. IR spectra were obtained at room temperature using a Jasco FT/IR-4100 with a diamond ATR setup.

Synthesis of $Eu(C_{15}H_{11}N_3)(H_2O)_2(NO_3)(Pt(CN)_4)\cdot CH_3CN$ (1). The synthesis of **1** was carried out by first mixing 1 mL of 0.12 M $Eu(NO_3)_3$ and 1 mL of 0.15 M $K_2[Pt(CN)_4]\cdot 3H_2O$. Next a 1 mL solution of 0.10 M 2,2′:6′,2″-terpyridine was layered onto the mixture. The $Eu(NO_3)_3$ and terpyridine solutions were prepared using CH_3CN as the solvent, while the $K_2[Pt(CN)_4]$ solution was made by dissolving $K_2[Pt(CN)_4]\cdot 3H_2O$ in a 20%:80% mixture of water/CH_3CN. Slow evaporation of the solvent over a period of 2 weeks resulted in the crystallization of **1** as colorless single crystals with a yield of 57.6%. IR(solid, cm^{-1}): 3244 (s, br), 2193 (w), 2185 (w), 2166 (w), 2148 (s), 1600 (m), 1580 (m), 1482 (s), 1451 (s), 1434 (s), 1422 (m, sh), 1304 (s), 1234 (m), 1196 (w), 1158 (m), 1075 (w), 1038 (m), 1015 (s), 813 (m), 768 (s).

Synthesis of $\{Eu(C_{15}H_{11}N_3)(H_2O)_3\}_2(Pt(CN)_4)_3\cdot 2H_2O$ (2). The synthesis of **2** was carried out by first mixing 1 mL of 0.10 M $Eu(CF_3SO_3)_3$ and 1 mL of 0.15 M $K_2[Pt(CN)_4]$. Next 1 mL of an 0.10 M 2,2′:6′,2″-terpyridine solution was layered on top. The terpyridine solution was prepared using CH_3CN as the solvent, while the $Eu(CF_3SO_3)_3$ and $K_2[Pt(CN)_4]$ solutions were prepared in 20%:80% solutions of water/CH_3CN. Slow evaporation of the solvent over a period of a week resulted in the crystallization of **2** as colorless single crystals with a yield of 44.4%. IR(solid, cm^{-1}): 3361 (s, br), 3100 (w, br), 2181 (w), 2160 (w, sh), 2142 (s), 1653 (m), 1647 (w), 1596 (s), 1575 (m), 1483 (m), 1460 (w, sh), 1450 (m), 1435 (s), 1399 (w), 1312 (m), 1268 (m), 1236 (m), 1196 (m), 1173 (w, sh), 1162 (s), 1078 (w), 1032 (m), 1013 (s), 904 (w), 771 (s), 742 (m), 669 (m).

Synthesis of $[Eu(C_{15}H_{11}N_3)(H_2O)_2(CH_3COO)_2]_2Pt(CN)_4\cdot 3H_2O$ (3). The synthesis of **3** was carried out by first mixing 1 mL of 0.10 M aqueous $Eu(CH_3COO)_3$ and 1 mL of 0.025 M $K_2[Pt(CN)_4]$. Next, a 1 mL solution of 0.10 M 2,2′:6′,2″-terpyridine was layered on top. The terpyridine solution was prepared using CH_3CN as the solvent, while the $K_2[Pt(CN)_4]$ solution was made by dissolving $K_2[Pt(CN)_4]\cdot 3H_2O$ in a 20%:80% mixture of water/CH_3CN. Slow evaporation of the solvent over a period of several days resulted in the crystallization of **3** as colorless single crystals with a yield of 63.9%. IR(solid, cm^{-1}): 3628 (m), 3550 (w, br), 3407 (w, br), 2134 (s), 2122 (s), 1616 (s), 1559 (m), 1456 (w), 1422 (m), 761 (m), 669 (m), 656 (m).

Single-Crystal X-ray Diffraction. Selected single crystals of **1**−**3** with dimensions of 0.476 mm × 0.268 mm × 0.078 mm, 0.460 mm × 0.166 mm × 0.120 mm, and 0.900 mm × 0.244 mm × 0.232 mm, respectively, were selected, mounted on quartz fibers, and aligned on an Enraf-Nonius CAD-4 single-crystal X-ray diffractometer with an optical microscope. Intensity measurements were performed using graphite monochromated Mo Kα radiation from a sealed tube. Three standard collections were collected every 2 h to monitor for crystal decay. The intensities of the reflections were collected using $\theta/2\theta$ scans.

All of the crystals examined in these studies diffracted extremely well and were non-problematic in regards to data collection and structure analysis. XCAD4[40] was used to process the raw X-ray data. The program suite SHELXTL (v 5.1) was used for space group determination and application of absorption corrections (XPREP), structure solution (XS), and least-squares refinement (XL).[41] The initial structure solutions were carried out using direct methods, and the remaining atomic positions were located in difference maps. For **1** and **3**, analytical absorption corrections were applied to the data, while a psi-scan absorption correction was applied for **2**. The final refinements included anisotropic displacement parameters for all non-hydrogen atoms. Some additional crystallographic details for **1**−**3** are listed in Table 1; further details of the crystal structure investigations may be found in the crystallographic files (cif format) supplied as Supporting Information.

Photoluminescence Measurements. The luminescence spectra were collected using a photon technology international (PTI) spectrometer (model QM-7/SE). The system uses a high intensity xenon source for excitation. Selection of excitation and emission wavelengths are conducted by means of computer controlled, autocalibrated "QuadraScopic" monochromators and are equipped with aberration corrected emission and excitation optics. Signal detection is accomplished with a PMT detector (model 928 tube) that can work either in analog or

(40) Harms, K.; Wocadlo, S. *XCAD4*; University of Marburg: Germany, 1995.

(41) Sheldrick, G. M. *SHELTXL PC, Version 5.0, An Integrated System for Solving, Refining, and Displaying Crystal Structures from Diffraction Data*; Siemens Analytical X-ray Instruments, Inc.: Madison, WI, 1994.

digital (photon counting) modes. All of the emission spectra presented are corrected to compensate for wavelength dependent variation in the system on the emission channel. The emission correction files which were generated by comparison of the emission channel response to the spectrum of a NIST traceable tungsten light were used as received from Photon Technology International (PTI). The emission correction was conducted in real time using the PTI provided protocol. The instrument operation, data collection, and handling were all controlled using the advanced FeliX32 fluorescence spectroscopic package. The steady state emission and excitation spectra were collected upon continuous excitation (without introducing any time delay). For the lifetime measurements various time delays were introduced ranging from 40 to 120 μs for the f-f emission, and 2−20 μs for the donor emission of **3**. All of the spectroscopic experiments were conducted on neat crystalline samples held in sealed quartz capillary tubes. The low temperature measurements were conducted on samples inserted in a coldfinger Dewar flask filled with liquid nitrogen.

Results and Discussion

Syntheses. The reactions of Eu^{3+} solutions with $K_2Pt(CN)_4 \cdot 3H_2O$ and 2,2′:6′,2″-terpyridine in H_2O/acetonitrile mixtures at room temperature leads to the formation of **1**, **2**, or **3** depending on whether the nitrate, triflate, or acetate salts, respectively, of Eu^{3+} are employed. Past synthetic studies by others[42] have also probed anion dependence on structure formation.

The preparation of three europium/terpyridine/tetracyanoplatinate structure types using the different europium salts can be rationalized based on the ability of the anions to coordinate Eu^{3+}. On the basis of these studies the relative strength of coordination of Eu^{3+} can be ranked as acetate > nitrate ~ tetracyanoplatinate > triflate. This order agrees well with the known tendency of these anions to coordinate Eu^{3+}. Carboxylates are known to strongly coordinate the oxophilic Ln^{3+} cations.[43−45] In the absence of other strongly coordinating anions, nitrate is also known to coordinate the trivalent lanthanide cations such as in $Eu(terpy)(H_2O)(NO_3)_3$.[46] However, the very weakly coordinating triflate anion does not typically coordinate the trivalent rare earth cations in the presence of other ligands. For example, in $Eu(H_2O)_9(CF_3SO_3)_3$[47] the Eu^{3+} cation is coordinated by nine water molecules, and the triflate anions are present in the crystal structure as non-coordinated anions. The triflate anions involved in the synthetic reaction of **2** do not coordinate the Eu^{3+} in the compound or even crystallize in the structure as counteranions. These examples are not meant to imply that there is not some precedent for triflate to coordinate to Ln^{3+} cations; it is found to do so in some instances, for example, in $[Eu(tpa)(H_2O)_2(CF_3SO_3)_3]$[48] (tpa = tris(2-pyridylmethyl)amine), but such cases are the exception rather than the rule.

(42) Shatruk, M.; Chouai, A.; Dunbar, K. R. *Dalton Trans.* **2006**, 2184–2191.
(43) Ouchi, A.; Suzuki, Y.; Ohki, Y. *Coord. Chem. Rev.* **1988**, *92*, 29–43.
(44) (a) Cotton, S. A. In *Encyclopedia of Inorganic Chemistry*; King, R. B., Ed.; John Wiley: New York, 1994, p 3595.
(45) Oczko, G.; Starynowicz, P. *J. Mol. Struct.* **2005**, *740*, 237–248.
(46) Cotton, S. A.; Noy, O. E.; Liesener, F.; Raithby, P. R. *Inorg. Chim. Acta* **2003**, *344*, 37–42.
(47) Chatterjee, A.; Maslen, E. N.; Watson, K. J. *Acta Crystallogr., Sect. B* **1988**, *B44*(4), 381–386.
(48) Natrajan, L.; Pecaut, J.; Mazzanti, M.; LeBrun, C. *Inorg. Chem.* **2005**, *44*, 4756–4765.

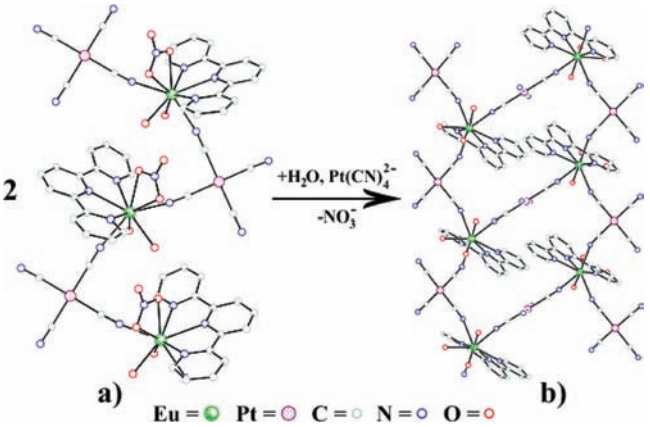

Figure 1. Representation of the 1-D chains in (a) **1** and (b) **2**.

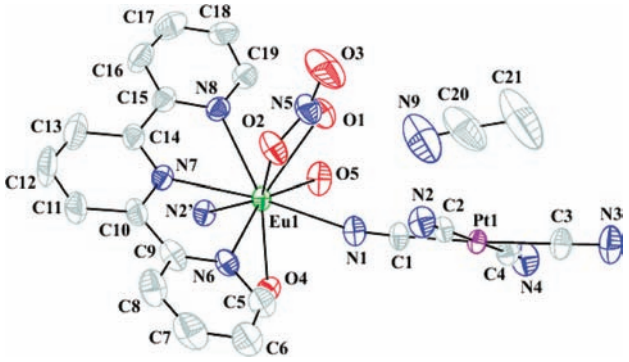

Figure 2. Thermal ellipsoid plot (50%) of **1** illustrating the coordination environment of the Eu site.

Table 2. Selected Bond Distances (Å) for $Eu(C_{15}H_{11}N_3)(H_2O)_2(NO_3)(Pt(CN)_4) \cdot CH_3CN$ (**1**)

Distances (Å)			
Eu1−N1	2.497(6)	Pt1−C1	1.974(6)
Eu1−N2′	2.509(5)	Pt1−C2	1.993(7)
Eu1−N6	2.578(5)	Pt1−C3	1.999(7)
Eu1−N7	2.579(5)	Pt1−C4	1.991(7)
Eu1−N8	2.571(6)	C1−N1	1.146(8)
Eu1−O1	2.577(5)	C2−N2	1.148(8)
Eu1−O2	2.482(5)	C3−N3	1.127(8)
Eu1−O4	2.390(5)	C4−N4	1.132(9)

Structural Studies. $Eu(C_{15}H_{11}N_3)(H_2O)_2(NO_3)(Pt(CN)_4) \cdot CH_3CN$ (1). The structure of **1** consists of neutral, 1-D $^1_\infty[Eu(C_{15}H_{11}N_3)(H_2O)_2(NO_3)(Pt(CN)_4)]$ chains. The chains are formed by the linkage of the Eu^{3+} cations by cis-bridging tetracyanoplatinate anions as shown in Figure 1a. The coordination of the sole crystallographic Eu site is 9-fold and can be described as a distorted $[EuO_4N_5]$ tricapped trigonal prism. The five nitrogen atoms in the inner sphere of the Eu^{3+} result from the coordination of one tridentate terpyridine ligand and two N-bound $Pt(CN)_4^{2-}$ anions while the four oxygen atoms are a result of one bidentate nitrate anion and two coordinated water molecules as shown in Figure 2.

A detailed list of the bond distances for **1** can be found in Table 2. The Eu−N and Eu−O bond distances range from 2.498(6) to 2.579(5) Å and 2.389(6) to 2.577(5) Å, respectively. The two longest Eu−O bond distances are those to the nitrate anion (average of 2.530(5)) while

the Eu−O distances to the coordinated water molecules are considerably shorter (2.404(6) Å average). These distances agree quite well with literature values; for example, the Eu−O bond distances to bidentate nitrate anions have average values of 2.517 and 2.515 Å in Eu(terpy)$(NO_3)_3(H_2O)$[46] (terpy = 2,2′:6′,2″-terpyridine) and Eu(bipy)$_2(NO_3)_3$[46] (bipy = 2,2′-bipyridine), respectively, and the Eu−O bond distances between Eu^{3+} and the coordinated water molecules in $Eu(H_2O)_9(CF_3SO_3)_3$[47] have an average value of 2.453 Å. A distinction in the distances for the Eu−N bonds to the cyano groups and the Eu−N bonds to the terpyridine moiety is also evident; the Eu−N bonds to the latter are longer by ∼0.07 Å. Comparison of these values with Eu−N distances found in Eu(terpy)$(NO_3)_3(H_2O)$[46] (2.554 Å average) and $\{K(DMF)_7Eu[Ni(CN)_4]_2\}$[22] (2.525(6) Å average) are consistent with the values for **1**. The Pt−C distances vary from 1.974(6) to 1.999(7) Å with an average of 1.989(7) Å. The C−N distances for the terminal cyano (1.129(9) Å average) groups are slightly shorter than for the bridging cyano groups (1.147(8) Å average) as also observed in other tetracyanoplatinate structures.[6,7a]

The packing diagram of **1** along the *c* crystallographic axis (parallel to the 1-D $^1_\infty[Eu(C_{15}H_{11}N_3)(H_2O)_2(NO_3)(Pt(CN)_4)]$ chains) is shown in Figure 3. Not shown in the packing diagram is the one molecule of acetonitrile per formula unit that crystallizes between the chains. The predominant interchain feature in the structure is the existence of Pt−Pt interactions. As described earlier,[49] these interactions have strengths comparable to hydrogen bonds and often direct the structures of compounds that contain them. The interchain Pt−Pt interactions in **1** have a distance of 3.5558(7) Å and result in the formation of Pt dimers. This is in contrast to what is normally observed in tetracyanoplatinate structural chemistry. The structures of TCP compounds are typically dominated by the presence of quasi-1-D stacks (also described as chains) of tetracyanoplatinate anions.[6] For example, $Er_2[Pt(CN)_4]_3\cdot 21H_2O$[7a] contains 1-D chains of tetracyanoplatinates anions which have non-equidistant Pt−Pt separations of 3.1625(5) and 3.1891(3) Å (average of 3.1758(8) Å) and $BaPt(CN)_4\cdot 4H_2O$[50] contains Pt−Pt distances of 3.321(3) Å in its stacks.

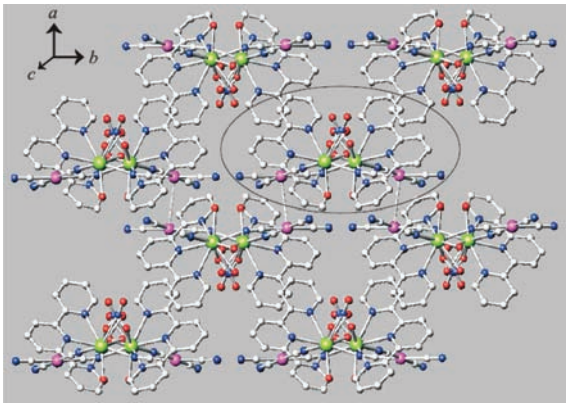

Figure 3. Packing diagram for **1** viewed along the *c* axis, the direction parallel to the 1-D chains. Pt−Pt interactions are shown by the dashed lines, and one of the 1-D chains is circled for clarity. Eu atoms are shown in green, Pt in purple, C in white, N in blue, and O in red.

$\{Eu(C_{15}H_{11}N_3)(H_2O)_3\}_2(Pt(CN)_4)_3\cdot 2H_2O$ (2). Like the structure of **1**, the structure of **2** is also 1-D in nature. However, it differs in that it consists of a neutral ladder structure with a formulation of $^1_\infty[\{Eu(C_{15}H_{11}N_3)(H_2O)_3)\}_2(Pt(CN)_4)_3]$. In contrast to **1**, the structure of **2** contains Eu^{3+} cations linked by both cis- and trans-bridging tetracyanoplatinate anions as shown in Figure 1b. Figure 1 is meant to illustrate how the chains in **2** are structurally related to the chains in **1**, and not to indicate that the synthesis of compound **2** has been achieved by reacting compound **1** with an additional tetracyanoplatinate anion. The compounds have only been formed through the two different synthetic routes described in the Experimental Section.

The coordination sphere of the one Eu^{3+} site in the structure of **2**, shown in Figure 4, contains one tridentate terpyridine ligand, three coordinated water molecules, and three N-bound cyano groups from the bridging tetracyanoplatinate moieties. The overall coordination environment of the Eu site is therefore nine and has a geometry that is nearly a regular tricapped trigonal prism. The Eu−N and Eu−O bond distances range from 2.508(6) to 2.594(6) Å and 2.449(5) to 2.529(6) Å, respectively. As also found in **1**, the three shortest Eu−N distances in **2** are to the tetracyanoplatinate anions; the Eu−N distances to the terpyridine moiety are ∼0.05 Å longer on average than the Eu−N distances to the $Pt(CN)_4^{2-}$ anions. The Eu−O distances to the coordinated water molecules in **2** are on average ∼0.09 longer than the equivalent Eu−O distances in **1**. The Pt−C distances vary from 1.966(9) to 2.000(8) Å with an average value of 1.985(8) Å. All of these bond distances are within normal ranges as found in previously reported lanthanide tetracyanoplatinates.[6,7a,21,22] Table 3 contains a more detailed list of the bond distances for **2**.

There are several similarities and also some significant differences in the 1-D structure found in **2** as compared with **1,** which can be seen in Figure 1. First, the chains in **2** are wider than those in **1** and can be viewed as two single

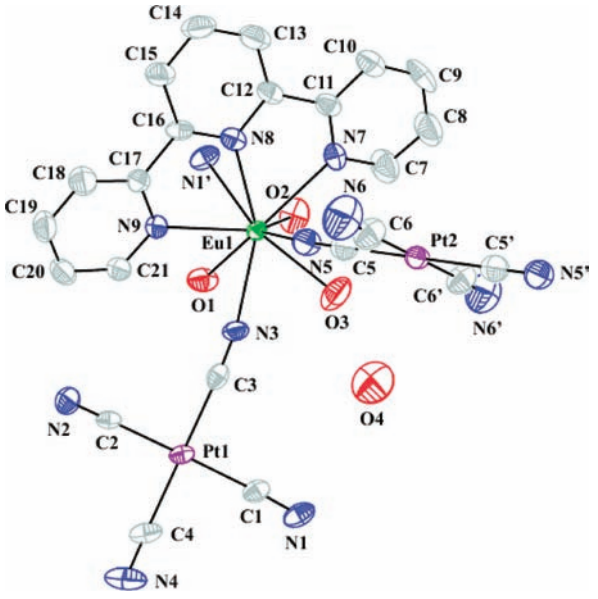

Figure 4. Thermal ellipsoid plot (50%) of **2** illustrating the coordination environment of the Eu site.

Table 3. Selected Bond Distances (Å) for $\{Eu(C_{15}H_{11}N_3)(H_2O)_3\}_2(Pt(CN)_4)_3 \cdot 2H_2O$ (**2**)

Distances (Å)			
Eu1−N1′	2.508(6)	Pt1−C3	1.994(8)
Eu1−N3	2.536(6)	Pt1−C4	1.987(8)
Eu1−N5	2.531(7)	Pt2−C5 (× 2)	2.000(8)
Eu1−N7	2.549(6)	Pt2−C6 (× 2)	1.966(9)
Eu1−N8	2.594(6)	C1−N1	1.146(9)
Eu1−N9	2.574(6)	C2−N2	1.146(10)
Eu1−O1	2.449(5)	C3−N3	1.141(10)
Eu1−O2	2.529(6)	C4−N4	1.141(11)
Eu1−O3	2.494(6)	C5−N5 (× 2)	1.139(10)
Pt1−C1	1.975(7)	C6−N6 (× 2)	1.160(12)

strands that are linked by a trans-bridging tetracyanoplatinate. This trans-bridging anion forms the rungs in the ladder structure of **2**. As also found in the packing diagram of **1**, the packing of the 1-D chains in **2** (Figure 5) does not result in quasi-1-D stacks of tetracyanoplatinate anions. Further, dimeric tetracyanoplatinate anions exist in **2** as also found in **1**, but the Pt1−Pt1′ interaction in **2** is considerably shorter with a value of 3.3967(6) Å. The Pt2 site does not form Pt−Pt interactions and the tetracyanoplatinate anion that contains it, the trans-bridging tetracyanoplatinate, is therefore "monomeric". It appears that the introduction of the bulky terpyridine unit in the structure of these tetracyanoplatinates results in sufficient structural distortion to disrupt the formation of the $Pt(CN)_4^{2-}$ stacks that were observed in earlier reported structures.[4a,6,7a] A similar situation has been observed in TCP salts containing large organic cations such as dianilinium[51] and 4,4′-bipiperidinium,[52] in which the structures contain discrete TCP anions.

$[Eu(C_{15}H_{11}N_3)(H_2O)_2(CH_3COO)_2]_2Pt(CN)_4 \cdot 3H_2O$ (3). The structure of **3** is molecular in nature and consists of two symmetry independent $[Eu(C_{15}H_{11}N_3)(H_2O)_2(CH_3COO)_2]^+$ complex cations crystallized with one $Pt(CN)_4^{2-}$ anion, as shown in Figure 6. In addition, three uncoordinated waters of hydration are also found in the structure. The distorted tricapped trigonal prismatic coordination geometries around each Eu^{3+} center result from one tridentate terpyridine ligand, two bidentate acetate anions, and two water molecules which provide a total of nine inner sphere atoms around the metal sites. In contrast to the structures of **1** and **2** described above, the $Pt(CN)_4^{2-}$ does not coordinate to the Eu^{3+} cation in **3**. The closest $Eu^{3+}/Pt(CN)_4^{2-}$ distance, between Eu1 and N9, is on the order of 4.516 Å. The large separation between these two groups in the structure has implications on the potential for energy transfer between them as described in the spectroscopic discussion below.

A detailed list of the important bond distances for **3** can be found in Table 4. The Eu−N and Eu−O bond distances in **3** range from 2.557(6) to 2.608(6) Å and 2.401(5) to 2.553(5) Å, respectively. Around the Eu(1) site, the

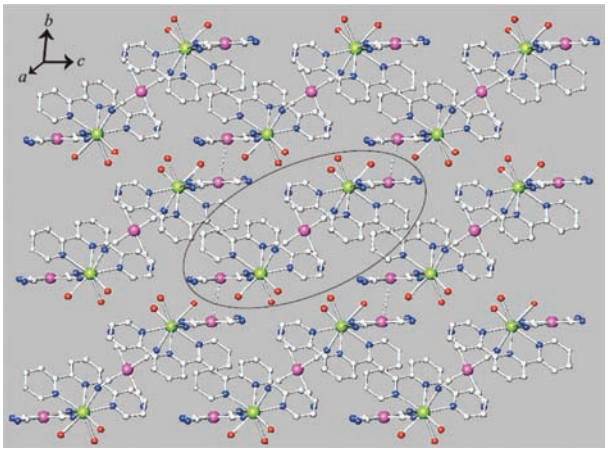

Figure 5. Packing diagram for **2** viewed along the *a* axis, the direction parallel to the 1-D chains. Pt−Pt interactions are shown by the dashed lines, and one of the 1-D chains is circled for clarity. Eu atoms are shown in green, Pt in purple, C in white, N in blue, and O in red.

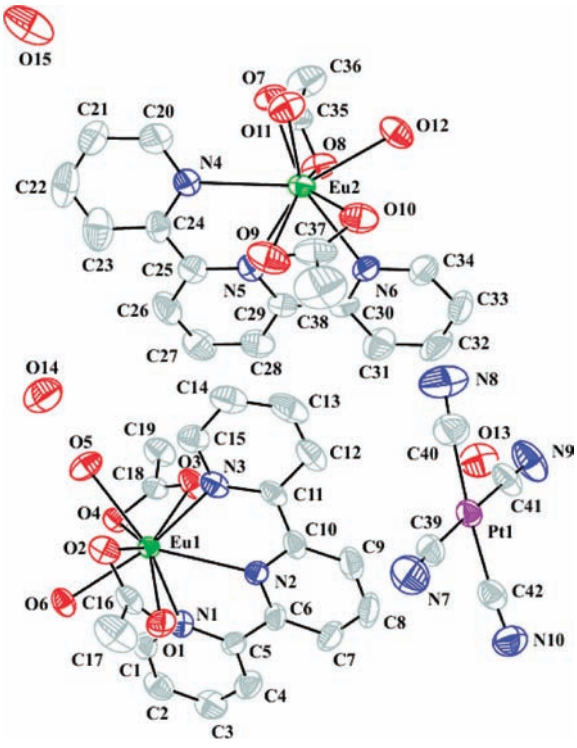

Figure 6. Thermal ellipsoid plot (50%) of **3** illustrating the coordination environments for the two crystallographic Eu sites and the non-coordinated tetracyanoplatinate anion.

average Eu−N and Eu−O bond distances are 2.585(6) and 2.457(5) Å, respectively, which are very close to the averages of 2.577(6) Å for Eu−N and 2.448(6) Å for Eu−O found for Eu(2). A trend in the distances for the Eu−O bonds to the acetate groups and the Eu−O bonds to the water molecules can not be made since these distances are overlapping. The Pt−C distances vary from 1.967(9) to 1.993(10) Å with an average of 1.982(10) and the average C−N distance is 1.15(1) Å. Compound **3** lacks Pt−Pt interactions; the shortest Pt−Pt distance in the compound is 9.076 Å.

Photoluminescence Studies. $Eu(C_{15}H_{11}N_3)(H_2O)_2(NO_3)(Pt(CN)_4) \cdot CH_3CN$ (1). The photoluminescence properties

(49) Xia, B.-H.; Zhang, H.-X.; Che, C.-M.; Leung, K.-H.; Phillips, D. L.; Zhu, N.; Zhou, Z.-Y. *J. Am. Chem. Soc.* **2003**, *125*, 10362–10374.
(50) Maffly, R. L.; Johnson, P. L.; Williams, J. M. *Acta Crystallogr., Sect. B* **1977**, *B33*(3), 884–887.
(51) Needham, G. F.; Johnson, P. L.; Williams, J. M. *Acta Crystallogr., Sect. B* **1977**, *B33*, 1581–1583.
(52) (a) Maynard, B. A.; Sykora, R. E. *Acta Crystallogr., Sect. E* **2008**, *E64*, m138–m139. (b) Crawford, P. C.; Gillon, A. L.; Green, J.; Orpen, A. G.; Podesta, T. J.; Pritchard, S. V. *CrystEngComm* **2004**, 419–428.

Table 4. Selected Bond Distances (Å) for $[Eu(C_{15}H_{11}N_3)(H_2O)_2(CH_3COO)_2]_2Pt(CN)_4 \cdot 3H_2O$ (**3**)

Distances (Å)			
Eu1−N1	2.564(6)	Eu2−N4	2.595(7)
Eu1−N2	2.608(6)	Eu2−N5	2.580(6)
Eu1−N3	2.582(6)	Eu2−N6	2.557(6)
Eu1−O1	2.417(5)	Eu2−O7	2.530(5)
Eu1−O2	2.524(5)	Eu2−O8	2.421(5)
Eu1−O3	2.421(5)	Eu2−O9	2.406(6)
Eu1−O4	2.553(5)	Eu2−O10	2.470(6)
Eu1−O5	2.426(5)	Eu2−O11	2.404(6)
Eu1−O6	2.401(5)	Eu2−O12	2.459(6)
Pt1−C39	1.976(8)	C39−N7	1.154(11)
Pt1−C40	1.992(11)	C40−N8	1.137(13)
Pt1−C41	1.967(9)	C41−N9	1.161(11)
Pt1−C42	1.993(10)	C42−N10	1.148(11)

Table 5. Excitation and Emission Data for $\{Eu(C_{15}H_{11}N_3)(H_2O)_3\}_2(Pt(CN)_4)_3 \cdot 2H_2O$ (**2**)

excitation bands			emission bands		
nm	cm^{-1}	assignment	nm	cm^{-1}	assignment
355	28200	$\pi-\pi^*$ (terpy)	454	22020	$^5D_2 \rightarrow {}^7F_1$
375	26700	CT $(Pt(CN)_4^{2-}$	527	18980	$^5D_1 \rightarrow {}^7F_0$
395	25300	$^5L_6 \leftarrow {}^7F_0$	536	18660	$^5D_1 \rightarrow {}^7F_1$
415	24100	$^5D_3 \leftarrow {}^7F_0$	556	17990	$^5D_1 \rightarrow {}^7F_2$
465	21500	$^5D_2 \leftarrow {}^7F_0$	580	17250	$^5D_0 \rightarrow {}^7F_0$
525	19050	$^5D_1 \leftarrow {}^7F_0$	591.4	16900	$^5D_0 \rightarrow {}^7F_1$
534	18700	$^5D_1 \leftarrow {}^7F_1{}^*$	595.6(d)	16790	$^5D_0 \rightarrow {}^7F_1$
			617.3 (s)	16200	$^5D_0 \rightarrow {}^7F_2$
			649	15400	$^5D_0 \rightarrow {}^7F_3$

* This band is absent in the low temperature spectrum indicating that thermal population from the ground $^7F_0$ state to the $^7F_1$ state precedes the optical transition.

of **1** were communicated earlier in greater detail.[39] Highlights of only some of the prominent features are discussed here, and figures containing the emission and excitation spectra are included as Supporting Information. A characteristic feature exhibited in **1** is a total absence of emission assignable to the $Pt(CN)_4^{2-}$ group, even at liquid nitrogen temperature, while sharp emissions characteristic of f-f transitions within the Eu^{3+} ion are dominant. The intensities of these bands increase significantly at 77 K. The excitation spectrum of **1** shows a broadband at ~350 nm, which is atypical of f-f transitions suggesting a donor/acceptor type interaction. An efficient IET process is inferred in this system since observance of a broad excitation band upon monitoring the Eu^{3+} emission is a direct evidence for donor/acceptor type energy transfer. On the basis of the excitation profile, it was concluded that both the terpyridine ligand and the metal-centered triplet state of $Pt(CN)_4^{2-}$ operate as sensitizers of the Eu^{3+} emission.[39]

$\{Eu(C_{15}H_{11}N_3)(H_2O)_3\}_2(Pt(CN)_4)_3 \cdot 2H_2O$ (2). Figure 7 shows the excitation spectra of **2**, monitored at the Eu^{3+} emission line at 617 nm. The profile is similar to that reported[39] for **1**. At both room and liquid N_2 temperatures the broadband at ~355 nm (with a shoulder at 375 nm) is dominant. The spectrum also displays sharp bands characteristic of Eu^{3+} ion f-f transitions, whose detail assignments are given in Table 5. In addition to the usual lowest ground $^7F_0$ level, a band originating from the higher $^7F_1$ level is also evident corresponding to the $^5D_1 \leftarrow {}^7F_1$ transition. This band is absent in the low temperature spectrum

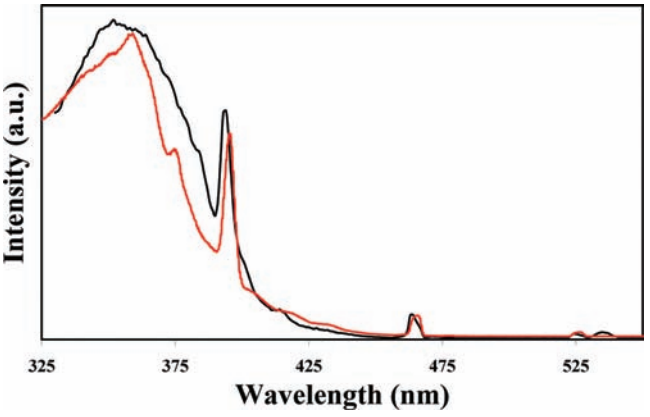

Figure 7. Excitation spectra of **2** collected at room temperature (black) and 77 K (red). Both spectra were collected by monitoring the Eu^{3+} emission line at 617 nm. Observance of the broad bands in the spectra is direct evidence for the existence of intramolecular energy transfer in **2**.

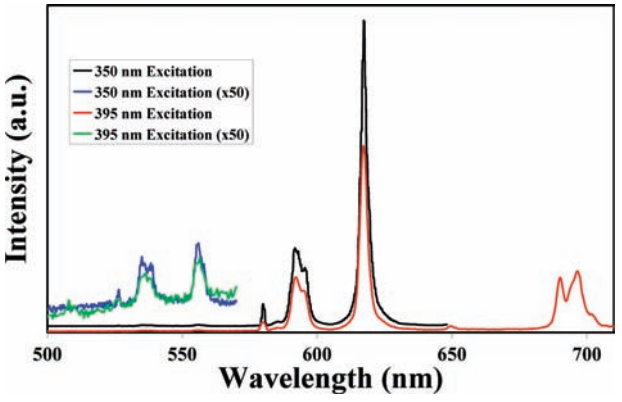

Figure 8. Emission spectra of **2** resulting from direct excitation at the Eu^{3+} ion f-f level at 395 nm or ligand-based excitation at 350 nm.

indicating that thermal population from the ground $^7F_0$ to the $^7F_1$ state precedes the optical transition.

The two emission spectra of **2** shown in Figure 8 were collected upon excitation at either 350 or 395 nm. The latter wavelength provides direct f-f excitation corresponding to $^5L_6 \leftarrow {}^7F_0$ transition. Apart from an intensity difference, the two spectra provided similar profiles. The series of sharp bands in the 580−702 nm range are typical of f-f transitions originating from the lowest $^5D_0$ excited state (Table 5). The $^5D_0 \rightarrow {}^7F_0$ transition shows a well-defined single peak at 580 nm corresponding to a single Eu^{3+} site in the lattice. The $^5D_0 \rightarrow {}^7F_1$ transition splits into two bands with a separation of 110 cm^{-1}. The $^5D_0 \rightarrow {}^7F_2$ transition at 617 nm is the most intense in the spectrum.

Close inspection of the emission profile reveals weak but sharp higher energy bands at 536 and 556 nm indicating the existence of more than one emitting state in the system. Both bands originate from the second excited state of Eu^{3+} and correspond to the $^5D_1 \rightarrow {}^7F_1$ and $^7F_2$ transitions, respectively.

The dominant broad excitation band shown in Figure 7 is centered at ~350−355 nm in the room temperature spectrum, which becomes sharper and red-shifts to 358 nm at 77 K. The low temperature spectrum also contains a well resolved shoulder on the longer

wavelength side at 375 nm. These bands are all uncharacteristic of f-f transitions. Like the situation observed in **1**, observance of Eu^{3+} ion emission upon excitation at 350 nm demonstrates that the sensitized emission from **2** is achieved through $Pt(CN)_4^{2-}$ based antenna triplet states and/or a terpyridine based $\pi-\pi^*$ intraligand transition.

The absorption profile of the "free" terpyridine ligand has a maximum at ~320 nm, with the tail of the band extending to 400 nm. The terpy ligand emits weakly at 385 nm and has an excitation maximum at ~340 nm. Comparison of the absorption spectrum of the ligand and excitation profiles of **2** indicates that the excitation maximum appears at the tail of the ligand absorption band.

In other Eu^{3+}/terpyridine systems where energy transfer processes have been reported[38] excitation maxima were observed in the 330−340 nm range. On the other hand, analysis of the excitation spectra of tetracyanoplatinate compounds indicates that these systems exhibit a broad excitation band in the 300−400 nm region, and in the absence of energy transfer are strongly luminescent in the visible region. For example, the lanthanum tetracyanoplatinate system studied by us[53] shows a broad yellow-green emission that maximizes at 515 nm and shows an excitation band in the 300−400 nm region. Although featureless at room temperature, the excitation band of this system at liquid nitrogen temperature shows a well-defined progression averaging ~2200 cm^{-1}. Hence, the transition is assignable to a CN coupled metal-to-ligand charge transfer transition. The gadolinium tetracyanoplatinate system,[53] also being studied by us, shows an excitation profile that extends up to 420 nm (with band maxima at ~340 and 410 nm).

Comparison of the profiles of the two sensitizer units, terpyridine and tetracyanoplatinate, clearly indicates that their excitation spectra overlap in the 300−400 nm region. The broad excitation band covering the near UV region in **2** indicates that sensitization proceeds both by the terpyridine ligand and the $Pt(CN)_4^{2-}$ anion, which are both directly coordinated to the Eu^{3+}. There is a total lack of emission corresponding to the $Pt(CN)_4^{2-}$ group in the visible region for both **1** and **2**, both at room and liquid nitrogen temperatures. The comparison is consistent with the argument presented earlier,[39] where the donor emission of the $Pt(CN)_4^{2-}$ is efficiently quenched because of energy transfer to the acceptor Eu^{3+} ion. In contrast, the donor groups reveal strong excitation bands upon monitoring the acceptor Eu^{3+} emission which can be taken as a direct evidence for the existence of energy transfer in the system.

$[Eu(C_{15}H_{11}N_3)(H_2O)_2(CH_3COO)_2]_2Pt(CN)_4\cdot 3H_2O$ (3). A major structural feature exhibited in **3** is the lack of direct bonding between the Eu^{3+} ion and the $Pt(CN)_4^{2-}$ group. As a result the donor/acceptor energy transfer process in **3** is significantly altered relative to **1** and **2**.

The photoluminescence spectra of **3** shown in Figure 9 (band locations and assignments given in Table 6) indicate that excitation at 340 nm provides only the characteristic Eu^{3+} emissions, albeit changing the excitation wavelength from 340 nm to longer wavelengths drastically changes the emission profiles. At 350 nm excitation, a weak broad emission emerges at ~500 nm, and its intensity increases systematically with an increase in the excitation wavelength, achieving a maximum intensity at ~390 nm excitation. Above 390 nm, the intensity of the broadband decreases with a concomitant reduction in the intensities of the sharper Eu^{3+} emissions. These changes are compared in Figure 9, and the dependence of the ratios of the emission intensities on excitation wavelength are shown in Figure 10.

(53) Assefa, Z.; Sykora, R. E., unpublished results.

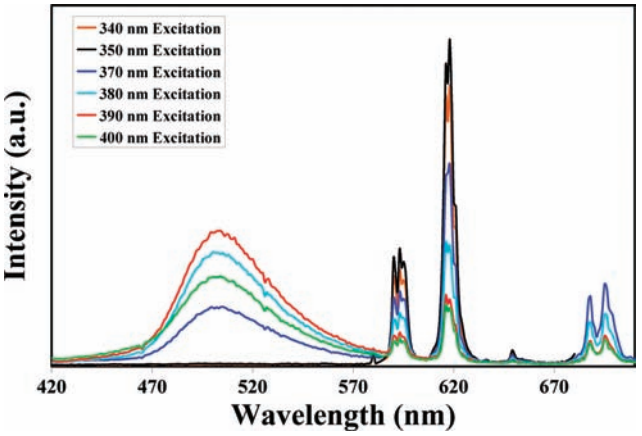

Figure 9. Emission spectra of **3** resulting from excitation at 340 nm, 350 nm, 370 nm, 380 nm, 390 nm, and 400 nm. Note that the Eu^{3+} emission is highly intensified upon excitation at 340 nm. All spectra were collected at room temperature.

Table 6. Excitation and Emission Data for $[Eu(C_{15}H_{11}N_3)(H_2O)_2(CH_3COO)_2]_2Pt(CN)_4\cdot 3H_2O$ (**3**)

excitation bands			emission bands		
nm	cm^{-1}	assignment	nm	cm^{-1}	assignment
350	28570	$\pi-\pi^*$ (terpy)	503	19870	$Pt(CN)_4^{2-}$
390	25640	CT $Pt(CN)_4^{2-}$	580	17240	$^5D_0 \rightarrow {}^7F_0$
395	25320	$^5L_6 \leftarrow {}^7F_0$	590	16950	$^5D_0 \rightarrow {}^7F_1$
465	21500	$^5D_3 \leftarrow {}^7F_0$	593	16860	$^5D_0 \rightarrow {}^7F_1$
526	19010	$^5D_2 \leftarrow {}^7F_0$	595	16810	$^5D_0 \rightarrow {}^7F_1$
535	18690	$^5D_1 \leftarrow {}^7F_1$	616	16230	$^5D_0 \rightarrow {}^7F_2$
538	18590	$^5D_1 \leftarrow {}^7F_1$	618	16180	$^5D_0 \rightarrow {}^7F_2$
			649	15400	$^5D_0 \rightarrow {}^7F_3$
			688	14530	$^5D_0 \rightarrow {}^7F_4$
			695	14390	$^5D_0 \rightarrow {}^7F_4$

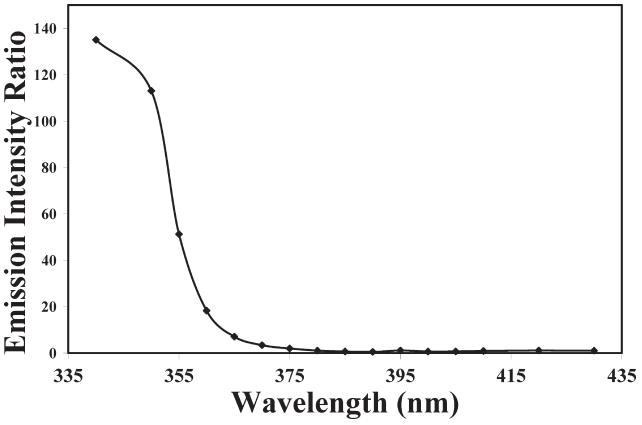

Figure 10. Dependence of the emission intensity ratio (616:500 nm) vs excitation wavelength for **3**.

As shown in these figures, the dependence of the emission profiles on the excitation wavelength is complex. The intensity ratio of the Eu^{3+} emission peak height and the broadband emission (616:500 nm) decreases drastically as the excitation wavelength changes from 340 nm to longer wavelengths. At 340 nm excitation, the intensity of the broad emission band is negligible, and the intensity ratio is 135. The ratio at 350 nm excitation is reduced to 113 and at 365 nm it is just 7. As the excitation wavelength is lengthened further to 380 and then to 390 nm the intensity ratio continues to drop, that is, 1.1 and 0.5, respectively. At 395 nm, however, the ratio increases slightly to 1.1 mainly because of the direct excitation of Eu^{3+} into the $^5L_6$ state. At excitation wavelengths longer than 395 nm, however, the ratio decreases, although the lowest ratio still corresponds to the 390 nm excitation.

These trends can be explained by an analysis of the excitation spectra of **3** shown in Figure 11. The spectrum shown in Figure 11a was collected by monitoring the Eu^{3+} ion emission at 617 nm. The spectrum consists of a broadband centered at ~350 nm that falls off sharply at the longer wavelength side, and has a shoulder on the shorter wavelength side. The characteristic Eu^{3+} f-f emissions are also evident in the spectrum. Figure 11b corresponds to the excitation spectrum monitored at the broad (500 nm) emission band. An entirely different excitation profile is observed, where a broadband that maximizes at ~390 nm dominates the spectrum. Clearly, the two excitation spectra behave as if two species are operating independently, which is consistent with the structural features of **3**. The TCP-based emission is totally quenched in both **1** and **2** because of efficient energy transfer processes within them. The lack of direct bonding between the tetracyanoplatinate anion and the Eu^{3+} ion in **3** appears to influence the spectral profile of **3**, where the energy transfer pathway from the TCP anion to the Eu^{3+} acceptor is blocked and the emission from the Pt $(CN)_4^{2-}$ moiety is observable at 500 nm.

The broad excitation band also contains a dip at 395 nm (Figure 11b). The dotted line in the figure is drawn to emphasize the correlation of the spectral dip with the 395 nm excitation band shown in Figure 11a. The presence of the dip indicates that part of the excitation energy at 395 nm is absorbed by the Eu^{3+} ion, reducing the intensity of the emission from the $Pt(CN)_4^{2-}$ group. Hence, the emission intensity drops when excited at 395 nm. This phenomenon appears to reflect the minimal interaction required for the observation of efficient nonradiative energy transfer between the two groups.

Although there appears to be minimal communication between the potential donor $Pt(CN)_4^{2-}$ group and the Eu^{3+} ion, we were able to observe the Eu^{3+} emission at all excitation wavelengths we used. Hence, additional analysis is warranted to help interpret this complicated data.

First, observance of the Eu^{3+} emission upon excitation at wavelengths shorter than 350 nm implies that strong excited state energy transfer exists between the terpy ligand and the Eu^{3+} ion. Such efficient energy transfer is expected since similar behavior was found in **1** and **2**. The sharp drop of the terpyridine excitation band past the 350 nm wavelength implies that the energy transfer efficiency decreases proportionately, hence the Eu^{3+} emission decreases as the excitation wavelength proceeds to longer wavelength. In contrast, the $Pt(CN)_4^{2-}$ emission increases in intensity as the excitation wavelength approaches a maximum value of 390 nm. At ~395 nm excitation, the Eu^{3+} emission is expected to increase since Eu^{3+} absorbs at this wavelength. Hence, a spectral dip is produced since a portion of this wavelength will be absorbed by Eu^{3+}, limiting the efficiency of excitation of the $Pt(CN)_4^{2-}$ unit. Close examination of the $Pt(CN)_4^{2-}$ emission band also provides evidence for other avenues of exciting the Eu^{3+} ion. The broad emission band shown in Figure 9b contains sharp dips at 465 and 526 nm. These dips correspond to $^5D_2$, $^5D_1 \leftarrow {}^7F_0$ transitions, respectively within the Eu^{3+} ion, a typical reabsorption phenomenon suggesting a radiative mechanism route responsible for the f-f emission. In summary, only the terpyridine moiety efficiently transfers its excited energy nonradiatively to the Eu^{3+} ion in **3**, while a radiative mechanism is evident from the $Pt(CN)_4^{2-}$ group.

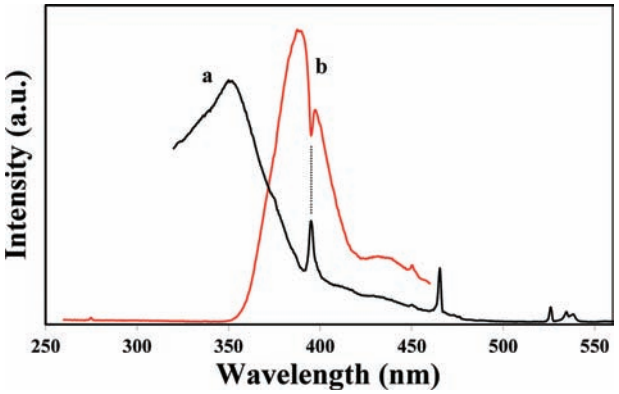

Figure 11. Excitation spectra of **3**. (a) Excitation spectrum monitored at the Eu^{3+} emission line at 617 nm. (b) Excitation spectrum monitored at the tetracyanoplatinate emission at 500 nm. Note the correlation between the dip in spectrum b and the 395 nm excitation band in spectrum a. The dotted line is drawn to guide the eye to this correlation.

Dual Donor Effect. Sensitization of lanthanide luminescence is traditionally achieved by π-conjugated organic aromatic chromophores that are directly coordinated to the metal centers.[35] An alternative approach for lanthanide sensitization is with transition-metal-containing antenna chromophores.[4a,36,37,54,55] One advantage afforded by the latter is a better energy match up between the d-block donors and the Ln^{3+} acceptor electronic levels.[4a] The energy match up between donor/acceptor levels results in less waste in excited energy. Some other added advantages include the relatively high triplet quantum yield obtained from the rapid intersystem crossing (due to the heavy-atom effect), and the facile detection of both quenching of the d-block chromophores and the sensitized emission from the lanthanide centers.[56]

The use of multiple donors for rational, systematic design of luminescent lanthanide probes is an area that needs to be developed since understanding the basic mechanisms of emission enhancement through a cooperative effect of

(54) McMillin, D. R.; Moore, J. J. *Coord. Chem. Rev.* **2002**, *229*, 113−121 and references therein.
(55) Glover, P. B.; Ashton, P. R.; Childs, L. J.; Rodger, A.; Kercher, M.; Williams, R. M.; De Cola, L.; Pikramenou, Z. *J. Am. Chem. Soc.* **2003**, *125*, 9918–9919.
(56) Li, X.-L.; Dai, F.-R.; Zhang, L.-Y.; Zhu, Y.-M.; Peng, Q.; Chen, Z.-N. *Organometallics* **2007**, *26*, 4483–4490.

multiple donor systems may lead to a rational design of materials useful for various applications.[28−34] One reported example in this area involves dual sensing/reporting capabilities that have been applied in dual-labeled probes with the potential use for genetic analysis to detect point mutations.[60] Only in a few cases has the concept of *dual-donor* been reported thus far.[57−59] For example, Kang et al. have reported the photophysical properties of an Er^{3+} system where the Er^{3+} ion is coordinated to mixed ligands consisting of terpyridine (terpy) and a Pt(II)-porphyrin derivative, Pt[5,10,15-triphenyl-20-(4-carboxyphenyl)-porphyrin] (PtP).[57a] The report indicated that both the PtP moiety and the terpy ligand contributed to the antenna effect, although the former has a dominant role in the energy transfer process. Faustino et al. also reported on a *dual-donor* system incorporating Eu^{3+} dithiocarbamate complexes containing various nitrogen donating ligands including 2,2′-bipyridine and 1,10-phenanthroline.[58] Emission enhancement, however, was limited in these systems because of the presence of a charge transfer state that competes effectively as a sink of the acceptor emission. Quici et al. reported a slightly different, but conceptually simpler system.[59] Their study consisted of a highly effective two component ligand system L, constituted from a *single* 1,10-phenanthroline (phen) chromophore. The phen ligand was flexibly linked via a methylene bridge to a 1,4,7,10-tetraazacyclododecane-1,4,7-triacetic acid unit. In this system effective luminescence sensitization was attained by protecting the coordination positions of the Ln^{3+} centers against solvent access. To the best of our knowledge no examples of *dual-donor* systems involving tetracyanoplatinate have been reported previously by other groups.

All three compounds studied in this work contain two potential sensitizers with overlapping excitation profiles. In compounds **1** and **2** the two donor species simultaneously enhance the acceptor emission. The two donors are the 2,2′:6′,2″-terpyridine ligand and the $Pt(CN)_4^{2-}$ anion, which are both directly coordinated to the acceptor lanthanide ion. The emission from the donor groups is totally quenched and only sensitized emission is observed from the acceptor Eu^{3+} ion.

In compound **3**, which lacks direct bonding between the $Pt(CN)_4^{2-}$ group and the acceptor Eu^{3+} ion, the sensitization involves only the terpy ligand. Hence, the spectral profiles lack coupling between the $Pt(CN)_4^{2-}$ group and the acceptor, Eu^{3+} ion. The two potential donor units operate independently providing totally different emission and excitation spectra. The little interaction present between the two involves a highly inefficient radiative mechanism, where reabsorption of the emission from the $Pt(CN)_4^{2-}$ provides weak emissions from the Eu^{3+} ion. Several of the excited states of the Eu^{3+} ion are involved in the radiative mechanism, including the $^5L_6$, $^5D_2$, and $^5D_1$ states, as inferred from the sharp dips contained in the emission band of the $Pt(CN)_4^{2-}$ units. Finally, although the donor−acceptor separation is within the Förster range, the overall spectral profile points to an inefficient process in the system.

Lifetime Studies. The lifetime of the $Pt(CN)_4^{2-}$ emission in **3**, measured at 500 nm, is 0.8 μs, consistent with several other tetracyanoplatinate systems that lack energy transfer (~0.25−1.5 μs[4a,61]). Although significant shortening of this lifetime would be expected upon nonradiative energy transfer, the donor emission is totally quenched in **1** and **2** precluding discernment of the energy transfer mechanism in these systems. For **3**, the large Stokes shift (~6400 cm^{-1}) between the excitation and emission maxima of the donor unit coupled with the μs lifetime indicates that the transition in $Pt(CN)_4^{2-}$ originates from the triplet excited state.

The acceptor Eu^{3+} ion emission has lifetimes of 420, 360, and 460 μs in **1**, **2**, and **3**, respectively. These differences can be attributed to the number of H_2O molecules directly coordinated to the Eu^{3+} ion in the different compounds.[62] In both **1** and **3** the number of water molecules directly coordinated are two, while **2** has three water molecules in the inner sphere of the Eu^{3+} ion.

An alternative explanation for this phenomenon is based on the suggestion of an anonymous reviewer. A recent paper by Puntus et al.[63] nicely explained the effect of H-bonding in facilitating energy transfer from ILCT to the acceptor Eu^{3+} ion ultimately resulting in emission enhancement. Of the three systems studied here, compounds **1** and **3** have the strongest H-bonding interactions (cif file in the Supporting Information) while **2** has the weakest interactions. As a result emission enhancement is expected in compounds **1** and **3** and by inference more quenching in compound **2**. The data is consistent with this analogy where the shortest lifetime corresponds to compound **2**, with the weakest H-bonding interactions.

Summary and Conclusions

Three different europium tetracyanoplatinates all incorporating 2,2′:6′,2″-terpyridine have been synthesized. Variation of the counteranion in the Eu^{3+} starting materials provided isolation of three distinct structure types. One-dimensional polymeric structure types were exhibited by **1** and **2**. The structure analysis of **3** revealed a zero-dimensional

(57) (a) Nah, M.-K.; Oh, J. B.; Kim, H. K.; Choi, K.-H.; Kim, Y.-R.; Kang, J.-G. *J. Phys. Chem. A* **2007**, *111*, 6157–6164. (b) Koullourou, T.; Natrajan, L. S.; Bhavsar, H.; Pope, S. J. A.; Feng, J.; Narvainen, J.; Shaw, R.; Scales, E.; Kauppinen, R.; Kenwright, A. M.; Faulkner, S. *J. Am. Chem. Soc.* **2008**, *130*, 2178–2179. (c) Pope, S. J. A. *Polyhedron* **2007**, *26*, 4818–4824. (d) Fernandes, M.; Nobre, S. S.; Goncalves, M. C.; Charas, A.; Morgado, J.; Ferreira, R. A. S.; Carlos, L. D.; Bermudez, V.; de, Z. *J. Mater. Chem.* **2009**, *19*, 733–742. (e) Woell, D.; Laimgruber, S.; Galetskaya, M.; Smirnova, J.; Pfleiderer, W.; Heinz, B.; Gilch, P.; Steiner, U. E. *J. Am. Chem. Soc.* **2007**, *129*, 12148–12158. (f) Picard, C.; Geum, N.; Nasso, I.; Mestre, B.; Tisnes, P.; Laurent, S.; Muller, R. N.; Elst, L. V. *Bioorg. Med. Chem. Lett.* **2006**, *16*, 5309–5312. (g) Yang, M.; Thompson, D. W.; Meyer, G. *J. Inorg. Chem.* **2000**, *39*, 3738–3739. (h) Eliseeva, S. V.; Kotova, O. V.; Gumy, F.; Semenov, S. N.; Kessler, V. G.; Lepnev, L. S.; Bünzli, J-C. G.; Kuzmina, N. P. *J. Phys. Chem. A* **2008**, *112*, 3614–3626.

(58) Faustino, W. M.; Malta, O. L.; Teotonio, E. E. S.; Brito, H. F.; Simas, A. M.; de Sa, G. F. *J. Phys. Chem. A* **2006**, *110*, 2510–2516.

(59) Quici, S.; Marzanni, G.; Cavazzini, M.; Anelli, P. L.; Botta, M.; Gianolio, E.; Accorsi, G.; Armaroli, N.; Barigelletti, F. *Inorg. Chem.* **2002**, *41*, 2777–2784.

(60) Xiao, Q.; Ranasinghe, R. T.; Tang, A. M. P.; Brown, T. *Tetrahedron* **2007**, *63*, 3483–3490.

(61) Weissbart, B.; Balch, A. L.; Tinti, D. S. *Inorg. Chem.* **1993**, *32*, 2096–2103.

(62) (a) Horrocks, W. D.Jr.; Sudnick, D. R. *Acc. Chem. Res.* **1981**, *14*, 384–392. (b) Frey, S. T.; Horrocks, W. de W.Jr. *Inorg. Chim. Acta* **1995**, *229*, 383–90.

(63) (a) Puntus, L.; Zhuravlev, K.; Lyssenko, K.; Antipin, M.; Pekareva, I. *Dalton Trans.* **2007**, 4079–4088. (b) Puntus, L. N.; Lyssenko, K. A.; Antipin, M. Yu.; Bünzli, J.-C. G. *Inorg. Chem.* **2008**, *47*, 11095–11107.

ionic compound containing two $[Eu(C_{15}H_{11}N_3)(H_2O)_2(CH_3COO)_2]^+$ cations and one $Pt(CN)_4^{2-}$ anion. It was revealed that the sensitization phenomena also vary drastically because of the structural differences. Compounds **1** and **2** display efficient donor−acceptor intramolecular energy transfer (IET) where dual donor species enhance the acceptor Eu^{3+} emission. In both compounds the terpyridine and tetracyanoplatinate donor species are directly coordinated to the Eu^{3+} ion, and hence a dual-donor effect is exhibited. In **3** where only the terpyridine donor is directly coordinated to Eu^{3+}, the sensitization only involves a terpy to Eu^{3+} IET mechanism. The $Pt(CN)_4^{2-}$ unit which lacks direct bonding in **3** exhibits a strong emission indicating the lack of cooperative enhancement of the Eu^{3+} emission.

Acknowledgment. R.E.S. gladly acknowledges ORNL and DOE for the loan of an X-ray diffractometer and USA for start-up funds. Z.A. acknowledges support from the NOAA Educational Partnership Program award number NA06OAR4810187 to NCAT State University and support from the ACS-PRF.

Supporting Information Available: Crystallographic data for **1**−**3** (CIF format) and photoluminescence spectra for **1**. This material is available free of charge via the Internet at http://pubs.acs.org.